Polymer Journal (2019) 51:861–868
https://doi.org/10.1038/s41428-019-0205-4

ORIGINAL ARTICLE

Dimensional properties of brush-like polymers with sodium Poly (styrene sulfonate) side chains

Yusuke Kitagawa[1] · Yusuke Hasegawa[1] · Keita Ide[1] · Yo Nakamura[1]

Received: 30 January 2019 / Revised: 26 March 2019 / Accepted: 31 March 2019 / Published online: 10 May 2019

Abstract

Brush-like polymer samples consisting of sodium poly(styrene sulfonate) were obtained by sulfonating polymacromonomers consisting of polystyrene with 110 monomeric units on each side chain. By fractional precipitation of the sample, fractions with narrow molecular weight distributions were obtained. Light scattering measurements were made to determine the mean-square radius of gyration for each fraction in aqueous NaCl as a function of the weight-average molecular weight and the salt concentration. By analyzing the data using the theory for the wormlike chain model, the stiffness parameters λ^{-1} of the molecule were obtained. It was found that the dependence of λ^{-1} on the salt concentration was not as strong as that for linear sodium poly(styrene sulfonate). This was interpreted as the reflection of the shielded charge–charge interactions at the local ionic strength in the brush which is much higher than that of the outside solution.

Introduction

Comb-like polymers with high side chain densities are called brush-like polymers. Typical brush-like polymers are obtained by the polymerization of macromonomers, which consist of a linear polymer with a polymerizable group at one of the chain ends. The resulting polymer is called a polymacromonomer (PM). It was shown that the main-chain stiffness of neutral PMs in organic solvents is much larger than that of linear polymers [1–6]. This enhanced stiffness was theoretically shown to arize from the repulsive interactions among side chains [7–11].

It is known that repulsive interactions between ionic polymer chains in aqueous media are much stronger than those of neutral polymers in organic solvents [12, 13]. Therefore, brush-like polymers with ionic side chains may have much higher stiffnesses in aqueous media. Rühe et al. [14] obtained several kinds of brush-like polymers with polyelectrolyte side chains. They showed that the cross-sectional diameters of quarternized poly(vinylpyridine) brushes and sulfonated polystyrene brushes determined by small-angle X-ray scattering were not very different from those of neutral brushes. However, they did not determine the stiffness parameter, λ^{-1}, of these polymers.

Previously, Kanemaru et al. [15] obtained PM samples with sodium poly(styrene sulfonate) (NaPSS) side chains by sulfonating PMs consisting of polystyrene (PS). They took light scattering and viscosity measurements of the solutions of NaPSS PM samples with the number of monomeric units, n_s, in the side chain at 15 and determined the mean-square radii of gyration and intrinsic viscosities in 0.05 M NaCl aqueous solution as functions of the molecular weight. Upon analyzing the data, they determined λ^{-1} and the diameter, d, of the polymer. It was shown that λ^{-1} for NaPSS PM is ~7.5 times larger than that for PS PM in toluene with the same n_s, while d for the former PM is ~1.1 times larger than that for the latter polymer. These results show that the effect of electrostatic interactions on λ^{-1} is very strong. On the other hand, the effects on d are not remarkable, confirming the results of Rühe et al. [14].

For further discussions of the electrostatic contributions to λ^{-1} and d, it may be important to study the dependence of these properties on the side chain length and the salt concentration, C_s. Here, we prepared NaPSS PM samples with n_s at ~110. Light scattering measurements were taken to determine the radius of gyration of each sample by changing the salt concentration. By analysis of the data, λ^{-1} and d were determined as functions of C_s.

✉ Yo Nakamura
yonaka@molsci.polym.kyoto-u.ac.jp

[1] Department of Polymer Chemistry, Kyoto University, Katsura, Kyoto 615-8510, Japan

Experimental procedure

Sample preparation

The NaPSS PM samples used in this study were obtained by the sulfonation of PS PM with side chains containing 113 (weight average) monomeric units [16]. Sulfonation was carried out by Vink's method [17] as follows. PS PM (1 g) dissolved in cyclohexane (50 cm^3) was slowly poured into conc. H_2SO_4 (33 cm^3) along with dissolved P_2O_5 (7.3 g) and stirred for 3 h at 40 °C. After 4 h, the solution was cooled to 0 °C, and ice (17 g) was added. At this time, some polymer was precipitated. The solution was transferred into a separable flask. After removing the acid phase, water was added to the flask, and it was shaken to dissolve the precipitated polymer. The water phase was separated from the organic phase, neutralized with NaOH aq., and poured into ethanol to precipitate the polymer. After drying in vacuo, the polymer was dissolved into water, and the solution was dialyzed against pure water for ~10 days. The water was changed every day. Dialysis was finished when the electric conductivity of the water phase no longer changed. Since the obtained samples had rather wide molecular weight distributions, each sample was fractionally precipitated with 1.0 M NaOH aq. as the solvent and ethanol as the precipitant. The central fraction was used for light scattering measurements. The fractionated samples dissolved in aqueous media were passed through a column packed with ion exchanging resin (Amberlite IR120B and Amberlite IRA400, Organo Co Ltd., mixed at 1:1). The obtained acid-type polymer was neutralized by NaOH aq. to the neutral point, taken as pH = 7.6 [18]. All the samples obtained were freeze-dried. The degree of sulfonation, f_s, for each sample was calculated from the weight ratio of C and S, as determined from the elemental analysis. The values are summarized in Table 1, along with the number-average to weight-average molecular weight ratios, M_w/M_n, determined by size-exclusion chromatography with the calibration curve for this PM. The molecular weight of the macromonomer, M_0, was calculated as 2.36×10^4 from the molecular weight of the macromonomer before sulfonation, considering full substitution.

Light scattering measurements

NaPSS PM samples were dissolved in NaCl aq. of a certain salt concentration, C_s. The solution was stirred for several days at room temperature when C_s was lower than 0.2 M and for more than one week when C_s was higher than 0.5 M. We tried to solve the polymer into NaCl aq. with C_s more than 2.0 M, but the polymer was not fully dissolved.

Light scattering measurements were taken by a multiangle light scattering detector (MALS), DAWN EOS (Wyatt Technologies, Inc.) with a laser of 690 nm wavelength. Each solution with a certain polymer concentration was slowly injected into the flow cell after passing through a hydrophilic poly(tetrafluoroethylene) filter with a 0.45 μm pore size. When the detector voltage became stable, the excess from the voltage for the solvent was taken as the excess scattering intensity of the solution. For each sample, five solutions with different polymer concentrations c were prepared for each C_s. To prevent saturation of the voltage, c was kept lower than 2.2×10^{-4} g cm^{-3} for samples SF110-5 and SF110-6 and lower than 1.0×10^{-4} g cm^{-3} for the other samples. At these concentration ranges, the concentration dependence of the scattering intensity divided by c was very small. Therefore, the second virial coefficient was not determined in this study.

The scattering intensities were extrapolated to $c \to 0$ using Berry's square-root plot to obtain $(Kc/R_\theta)_{c=0}$, where K is the optical constant and R_θ is the Rayleigh ratio at the scattering angle θ. The mean-square radii of gyration $\langle S^2 \rangle$ and M_w were determined from the slope and the intercept at $k^2 = 0$, respectively, for the plot of $(Kc/R_\theta)_{c=0}^{1/2}$ vs k^2, where k is the magnitude of the scattering vector.

The specific refractive index increment (dn/dc) of NaPSS sample SF110-4 was determined using Shimadzu differential refractometer at 436 and 546 nm wavelength, λ_0, at $C_s = 0.05$ and 0.20 M. Before the measurements, each solution was dialyzed against an NaCl solution with the same C_s as that used for the preparation of the solution. The results are as follows: 0.191 and 0.190 (cm^3 g^{-1}) for $C_s = 0.05$ and 0.20 M, respectively, at 436 nm and 0.185 and 0.183 (cm^3 g^{-1}) for $C_s = 0.05$ and 0.20 M, respectively, at 546 nm. The values at 690 nm were calculated from the linear relation between (dn/dc) and λ_0^{-2}, and those at different C_s values were calculated assuming a linear relation between (dn/dc) and C_s.

Table 1 Properties of polymacromonomer samples consisting of sodium Poly(styrene sulfonate)

Sample	10^{-5} M_w	M_w/M_n	f_s
SF110-1	530	–	1.0_4
SF110-2	60.7	1.10	1.0_1
SF110-3	25.5	1.14	1.0_0
SF110-4	14.1	1.27	0.99
SF110-5	9.29	1.02	1.0_0
SF110-6	5.28	–	1.0_2

Results

Light scattering data

Figure 1 shows plots of $(Kc/R_\theta)_{c=0}^{1/2}$ vs k^2 for SF110 samples in 0.05 M NaCl aq. From the intercept at $k^2 = 0$ and the

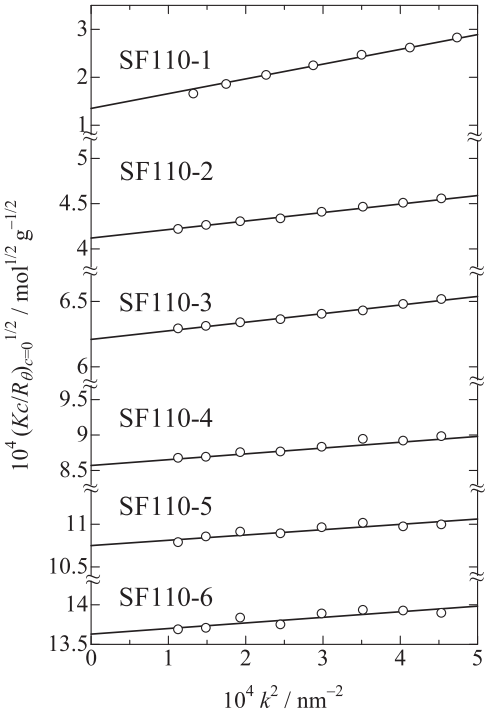

Fig. 1 Square-root reciprocal excess scattering intensities plotted against the square of the magnitude of the scattering vector for SF110 samples in 0.05 M NaCl aq

slope of each line fitted to the data, M_w and $\langle S^2 \rangle$ were determined.

All the data of $\langle S^2 \rangle$ for the NaPSS PM in different C_s are summarized in Table 2, along with the M_w values. Since the M_w values at different C_s values agreed within ±6.5%, the averaged value for each sample is indicated. The C_s dependence of $\langle S^2 \rangle$ for the five samples is shown in Fig. 2. The figure shows that $\langle S^2 \rangle$ monotonically decreases with increasing C_s, which is consistent with the $\langle S^2 \rangle$ of linear NaPSS in NaCl aq. However, the C_s dependence of NaPSS PM is much weaker than that of linear NaPSS [19].

Fig. 3 shows $\langle S^2 \rangle$ at $C_s = 0.05$ M plotted against the degree of polymerization of the macromonomer N_w, which was calculated from M_w/M_0. In the figure, data for PS PM with the same side chain length in toluene [16] are also shown. The figure shows that the $\langle S^2 \rangle$ values for NaPSS PM are much larger than those for PS PM when N_w is less than 10^2. However, the values for the former polymer approach those for the latter polymer at higher N_w values. This is very different from the case for NaPSS PM with shorter side chains. In the cases of NaPSS PM and PS PM with side chains of 15 monomeric units (SF15 and F15, respectively), the $\langle S^2 \rangle$ values for both polymers are close when N_w is less than 10^2, but the values for SF15 become much larger than those for F15 with increasing N_w [15].

Table 2 Radii of gyration of polymacromonomers consisting of sodium Poly(styrene sulfonate)

C_s/M	10^{-2} $\langle S^2 \rangle$ (nm^2)					
	SF110-1	SF110-2	SF110-3	SF110-4	SF110-5	SF110-6
0.005	218	13.9	5.9	5.6	3.6	3.3
0.01	–	13.7	6.2	5.8	3.8	–
0.05	137	13.7	6.3	5.7	3.5	3.1
0.20	–	12.4	5.3	5.1	3.2	–
0.50	111	12.2	5.3	4.8	3.6	2.4
0.00	93	12.0	5.0	4.6	3.0	–

Fitting data

In Fig. 4, the molecular dependence of $\langle S^2 \rangle$ at different C_s values is shown by different symbols. The solid lines show the values calculated from the following equation [20, 21]:

$$\langle S^2 \rangle = \frac{L}{6\lambda} - \frac{1}{4\lambda^2} + \frac{1}{4\lambda^3 L} - \frac{1}{8\lambda^4 L^2}[1 - \exp(-2\lambda L)] + \frac{d^2}{8} \quad (1)$$

for the wormlike chain with the diameter d. Here, the contour length, L, of the polymer is calculated from [22]

$$L = M_w/M_L + \delta \quad (2)$$

with the apparent contribution δ of the side chains near the main chain ends to L. Kanemaru et al. [15] reported that the contour length per repeating unit of the main chain, h, is 0.26_5 for SF15 when determined from the $\langle S^2 \rangle$ data. Using this h and M_0, M_L is estimated as 8.91×10^4 nm^{-1}. The solid line in the figure shows the calculated values with λ^{-1}, d, and M_L, where d and δ are assumed to be equal. Although the agreement between the experimental and calculated values is moderate, we may estimate the wormlike chain parameters from the fitting results.

The obtained parameters are summarized in Table 3.

Discussion

Diameter of the molecule

The chain diameter d of NaPSS PM at $C_s = 0.05$ M is plotted against the number of monomeric units in a side chain, n_s, in Fig. 5, denoted by the unfilled circles. The figure also includes the data for PS PM in toluene, shown as the filled circles [6, 16, 23]. The values for NaPSS PM are larger than those for PS PM, and the difference becomes larger with increasing n_s.

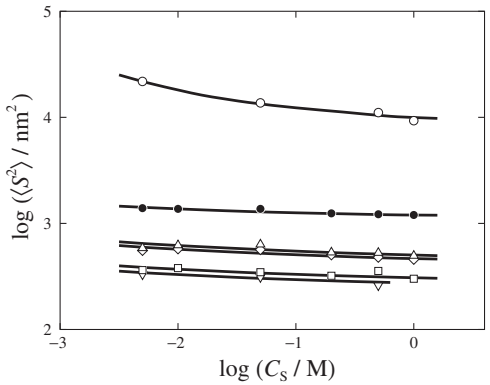

Fig. 2 Salt concentration dependence of the radius of gyration for SF110 samples (unfilled circles, SF110-1; filled circles, SF110-2; upward triangles, SF110-3; diamonds, SF110-4; squares, SF110-5; downward triangles, SF110-6)

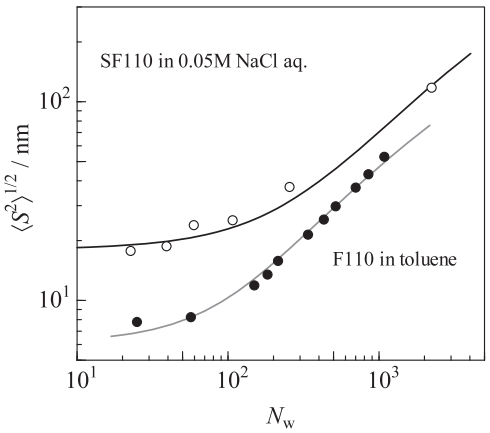

Fig. 3 Radii of gyration of SF110 in 0.05 M NaCl aq. (unfilled circles) and F110 in toluene (filled circles) plotted against the weight-averaged degree of polymerization of the main chain

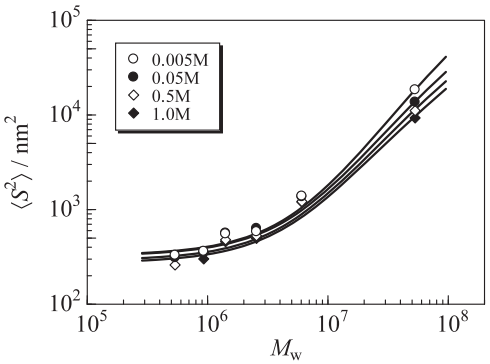

Fig. 4 Molecular weight dependence of the radius of gyration of SF110 at various salt concentrations. Solid lines show the theoretical fitting based on Eq. (1)

Table 3 Stiffness parameter and diameter for polymacromonomer SF110

C_s/M	d/nm	λ^{-1}/nm
0.005	41 ± 4	380 ± 40
0.05	40 ± 4	210 ± 20
0.50	40 ± 4	140 ± 15
0.00	38 ± 4	120 ± 10

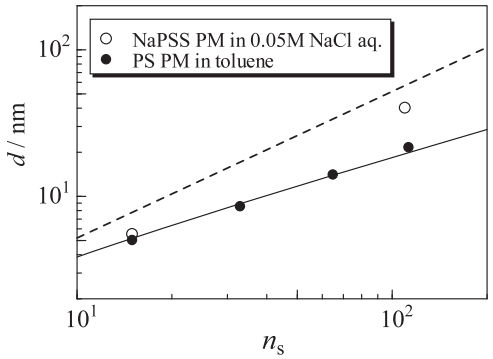

Fig. 5 Molecular diameter plotted against the number of monomeric units in a side chain for NaPSS PM in 0.05 M NaCl aq. (unfilled circles) and PS PM in toluene (filled circles). The solid and dashed lines show the end-to-end distance of the wormlike chain model with parameters for NaPSS [26] and that of the full stretching chain, respectively, with a length twice as long as the side chain of PM

The diameter of a brush-like polymer molecule may be comparable to the end-to-end distance of the linear polymer with a length twice as long as its side chain. The solid line in the figure represents the values for the end-to-end distance, $\langle R^2\rangle^{1/2}$, of the NaPSS chain calculated from the following equation:

$$\langle R^2\rangle = \langle R^2\rangle_0 \alpha_R^2 \tag{3}$$

where $\langle R^2\rangle_0$ indicates the mean-square end-to-end distance of the unperturbed wormlike chain and α_R is the end-to-end distance expansion factor. The quasi-two-parameter scheme [24] with the Domb–Barrett equation [25] was used for the calculation of α_R, with the wormlike chain parameters for the NaPSS chain in 0.05 M NaCl aq. of $M_L = 800$ nm, $\lambda^{-1} = 5.0$ nm, and $B = 4.0$ nm [26]. The solid line is rather close to the values for PS PM. In particular, the value for NaPSS PM with $n_S \sim 2 \times 10^2$ (the present study) is much larger than the values given by the solid line and those for PS PM in toluene. This suggests that the NaPSS side chains of SF110 are much more extended by the repulsive interactions from the surrounding side chains.

The dashed line shows the end-to-end distance of the fully stretched linear PS chain with a length twice as long as

the side chain in the zigzag state. The values for NaPSS PM are rather close to this line, showing that the side chains are almost fully stretched by the repulsive interactions among the side chains.

Stiffness parameter

The dependence of λ^{-1} on n_s for NaPSS PM at $C_S = 0.05$ M is shown in Fig. 6, along with the data for PS PM in toluene. The figure shows that the values of λ^{-1} for both polymers increase with increasing n_s, although the dependence of NaPSS PM is much weaker than that of PS PM.

The dashed and dotted lines in the figure show the calculated values for brush-like polymers having Gaussian side chains [10] with the excluded-volume parameters for NaPSS [24] and PS [27], respectively, in the corresponding solvents. Although the data for PS PM are close to the dotted line, the n_s dependence of the data for NaPSS PM is very different from the dashed line. Since the λ^{-1} of the brush-like polymers with rod-like side chains have the same n_s dependence as that of brush-like polymers with Gaussian side chains [28], the disagreement between the NaPSS data and the dashed line may not be ascribed to the side chain conformation but to the approximation of the short-range interaction.

In Fig. 7, the λ^{-1} of SF110 is plotted against C_s, where λ^{-1} gradually decreases with increasing C_s. Here, we consider the following model to calculate the stiffness parameter of the main chain of the brush-like polymer with polyelectrolyte side chains. For simplicity, the side chains are assumed to be straight and connected perpendicularly to the main chain with an equal spacing, h. Each side chain has an array of charges with equal spacing. By Manning's counterion condensation hypothesis [29], counterions bind to the charged groups on the polymer chain when the charge spacing is less than the Bjerrum length, Q_B. Because the real charge spacing of our polymer is about one third of the Q_B, the effective number, n_s', of the charged groups in a side chain becomes about one third of n_s. The left effective charges are assumed to interact with each other according to the Debye–Hückel potential [30]. The free energy per molecule is obtained by summing the potentials for all the pairs of the charged groups. By calculating the difference between the free energy before and after bending the main chain to a certain curvature from the straight state, the stiffness parameter was obtained (see Appendix for details).

The calculated values are shown by the dotted line in Fig. 7. The theory predicts too much strong dependence of λ^{-1} on C_s. In this theory, we do not consider the local ionic strength in the brush. For brush-like polymers consisting of side chains with ionic groups, the local concentrations of small ions in the brush may be far different from those outside the

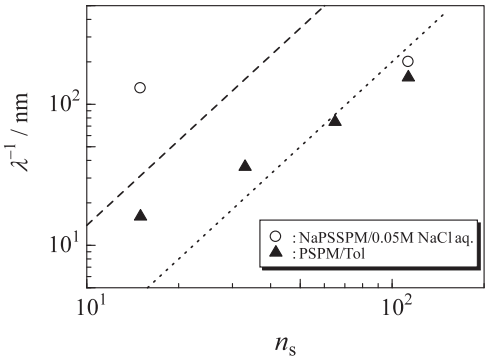

Fig. 6 Stiffness parameters for NaPSS PM in 0.05 M NaCl aq. (circles) and PS PM in toluene (triangles) plotted against the number of monomeric units in a side chain. The dashed and dotted lines show the calculated values for brush-like polymers consisting of Gaussian side chains with excluded-volume parameters for NaPSS and PS, respectively

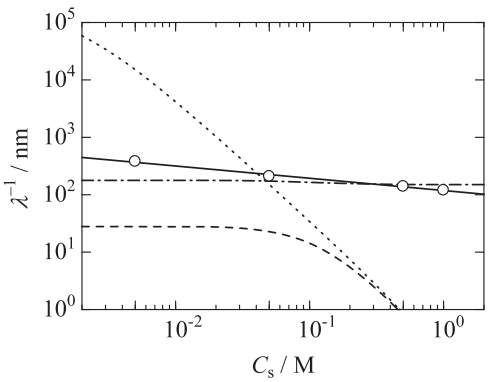

Fig. 7 The stiffness parameter for SF110 in NaCl aq. plotted against the salt concentration (circles). The solid line is the eye guide and the other lines are the calculated values (see text)

brush. Since the concentration of the ionic groups of the side chains is higher than that in the outside solution, the ionic strength inside the brush must also be higher than that outside the brush. To calculate this value, the Donnan equilibrium theory [31] may be applicable.

If the chemical potentials of the ionic salt inside and outside of the brush are in equilibrium, we may write

$$m_+' m_-' \gamma_\pm' = m_+ m_- \gamma_\pm \tag{4}$$

Here, m_+ and m_- mean the concentrations of positive and negative ions in the outside solution, respectively, $\gamma_\pm$ expresses the mean activity coefficient of the ions, and the prime designation means the value inside the brush. Here, the difference between the activity coefficients inside and outside of the brush is ignored by an approximation. The local concentration of the ionic groups on the side

chains, m_p, may be calculated by

$$m_p = \frac{n_s'}{\pi(d/2)^2 h} \quad (5)$$

By the neutrality condition,

$$m_+' = m_p + m_-', \quad m_+ = m_-(= C_s) \quad (6)$$

From these equations, m_+', m_-', and ionic strength or the Debye length inside the brush at each C_s were calculated with $d = 39$ nm (the averaged value) and $h = 0.26$ nm. Then, we calculated λ^{-1} by assuming that the charges on the brushes interact in the ionic atmosphere with this ionic strength. The calculated results are shown by the dashed line in Fig. 7. They are much lower than the dotted line for $C_s \lesssim 0.1$ and approach the line at larger C_s value. The calculated values for $C_s \lesssim 0.05$ are almost constant but are about one order smaller than the experimental values. The difference between the calculated and experimental values may be attributed to the interactions without the electrostatic interactions. Such interactions may be denoted as nonelectric interactions. If we express the contribution from the electrostatic interactions and the nonelectric interactions by λ_{el}^{-1} and λ_{ne}^{-1}, respectively, we may write

$$\lambda^{-1} = \lambda_{ne}^{-1} + \lambda_{el}^{-1} \quad (7)$$

The dot-dashed line shows the calculated value with λ_{el}^{-1} of the long-dashed line using $\lambda_{ne}^{-1} = 150$ nm, which was chosen to allow the calculated values to be close to the experimental values. The figure indicates that the stiffness parameter of this polymer is dominated by the constant term λ_{ne}^{-1}. We note that the value of λ_{ne}^{-1} is close to λ^{-1} for the polystyrene polymacromonomer with the same side chain length in toluene. However, the agreement may be accidental because the conformations of the side chains before and after sulfonation are very different. The weak dependence of the observed λ^{-1} on C_s may be due to the changes of the distribution of the ions in the brush with the change of C_s.

We may also calculate λ_{el}^{-1} for SF15 at $C_s = 0.05$ M by a similar procedure. Without considering the Donnan equilibrium between the inside and outside the brush, we obtained $\lambda_{el}^{-1} = 97$ nm. However, if we consider the Donnan equilibrium with $d = 5.5$ nm, the value is reduced to $\lambda_{el}^{-1} = 0.40$ nm, which is much smaller than the experimental value. For λ^{-1} of this polymer, the contribution of the nonelectric interaction must also be dominant. For further discussion, data on the salt concentration dependence of λ^{-1} for NaPSS PM with different side chain lengths may be necessary.

Conclusion

In this paper, we determined the stiffness parameter λ^{-1} of a brush-like polymer with side chains consisting of ~110 sodium styrene sulfonate monomeric units in aqueous NaCl. The dependence of λ^{-1} on the salt concentration was much weaker than that for linear sodium poly(styrene sulfonate) and the prediction of the theory considering the Debye–Hückel potential between charges on the side chains. It was shown that the high ionic strength in the brush modifies the ionic atmosphere and suppresses the interaction among charged groups. To obtain a quantitative agreement between the observed and theoretical values, the contribution from the nonelectric interactions among side chains without the electrostatic interactions have to be considered.

Acknowledgements We thank Professor Takenao Yoshizaki of Kyoto University for valuable discussion.

Compliance with ethical standards

Conflict of interest The authors declare that they have no conflict of interest.

Appendix

Calculation of the stiffness parameter for the main chain of brush-like polymers containing rod-like side chains with electrostatic interactions

If the Debye–Hückel potential is assumed for the electrostatic interaction between the ith and the jth charges on the different side chains p and q, the potential, w_{ij}, between the two charges is described as [30]

$$\frac{w_{ij}}{k_B T} = Q_B \frac{e^{-\kappa r_{ij}}}{r_{ij}}$$

Here, Q_B is the Bjerrum length and κ is the reciprocal of the Debye length. The indices i and j run from 1 to n_s' from the (effective) charge closest to the junction point to the farthest one. The the distance r_{ij} between the ith and the jth charges before bending the main chain is represented by

$$r_{ij}^2 = (jb\cos\phi_q - ib\cos\phi_p)^2 + (jb\sin\phi_q - ib\sin\phi_p)^2 + (q-p)^2 h^2$$

Here, the main chain is assumed to be on the z axis. In the above equation, h and b indicate the spacings of the junction points and of the charges on the side chain,

respectively. ϕ_p and ϕ_q denote the rotating angle of the pth and qth side chains, respectively, from the xz plane (see Figure 8).

When the main chain is bent in the xz plane with the radius of curvature R_c, r_{ij} is changed to r'_{ij}, as given by the following equation,

$$r'^2_{ij} = r^2_{ij} + \theta^2_{pq} ijb^2 \cos\phi_p \cos\phi_q - \theta^2_{pq} R_c (ib\cos\phi_p + jb\cos\phi_q) - \theta^4 R_c^2/12$$

if we consider up to the order of R_c^2. Here, θ_{pq} is the angle made by the pth and the qth junction points on the main chain around the center of the curvature and is given by

$$\theta_{pq} = (q-p)h/R_c$$

The change in the potential energy, Δw_{ij}, by bending the main chain can be calculated as

$$\frac{\Delta w_{ij}}{k_B T} = Q_B \left\{ e^{-\kappa r_{ij'}}/r_{ij'} - e^{-\kappa r_{ij}}/r_{ij} \right\} = \frac{Q_B}{24 R_c^2}(q-p)^4 h^4 \left\{ \frac{\kappa}{r_{ij}^2} + \frac{1}{r_{ij}^3} + \frac{3\kappa}{r_{ij}^4 (i^2+j^2) b^2} \right\} e^{-\kappa r_{ij}} \quad (8)$$

Here, Δw_{ij} was averaged over ϕ_p and ϕ_q, assuming that the direction of the side chain around the main chain is random. By this assumption, r_{ij} may be replaced by the averaged value, $\overline{r}_{ij}$, over ϕ_p and ϕ_q:

$$\overline{r}_{ij} = (i^2+j^2)b^2 + (q-p)^2 h^2$$

The change in the total free energy of the molecule is given by,

$$\Delta F = \sum_{p<q} \sum_i \sum_j \Delta w_{ij}$$

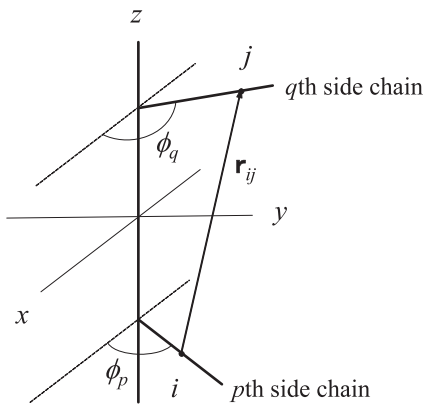

Fig. 8 Geometry of a brush-like polymer molecule consisting of straight side chains with charged groups

The effective stiffness parameter of this molecule is given by,

$$\lambda_{\text{eff}}^{-1} = \frac{4R_c^2}{L}\frac{\Delta F}{k_B T}$$

Considering the Manning counterion condensation theory, we assumed that the effective interval of the charges, b, on each side chain is equal to Q_B. Since $\lambda_{\text{eff}}^{-1}$ at each C_s depended on the number of side chains N, we plotted $\lambda_{\text{eff}}^{-1}$ against N^{-1} and extrapolated to $N^{-1} = 0$ to obtain λ_{el}^{-1}.

References

1. Wintermantel M, Schmidt M, Tsukahara Y, Kajiwara K, Kohjiya S. Rodlike combs. Macromol Rapid Commun. 1994;15:279–84.
2. Nemoto N, Nagai M, Koike A, Okada S. Diffusion and sedimentation studies on Poly(macromonomer) in dilute solution. Macromolecules. 1995;28:3854–9.
3. Wintermantel M, Gerle M, Fischer K, Schmidt M, Wataoka I, Urakawa H, et al. Molecular bottlebrushes. Macromolecules. 1996;29:978–83.
4. Kawaguchi S, Akaike K, Zhang Z-M, Matsumoto H, Ito K. Water soluble bottlebrushes. Polym J. 1998;30:1004–7.
5. Terao K, Takeo Y, Tazaki M, Nakamura Y, Norisuye T. Polymacromonomers consisting of polystyrene. Light scattering characterization in cyclohexane. Polym J. 1999;31:193–8.
6. Terao K, Nakamura Y, Norisuye T. Solution properties of polymacromonomer consisting of polystyrene. 2. Chain dimensions and stiffness in cyclohexane and toluene. Macromolecules. 1999;32:711–6.
7. Fredrickson GH. Surfactant-induced lyotropic behavior of flexible polymer solutions. Macromolecules. 1993;26:2825–31.
8. Zulina EB, Vilgis TA. Scaling theory of planner brushes formed by branched polymers. Macromolecules. 1995;28:1008–15.
9. Subbotin A, Saariaho M, Ikkala O, ten Brinke G. Elasticity of comb copolymer cylindrical brushes. Macromolecules. 2000;33:3447–52.
10. Nakamura Y, Norisuye T. Backbone stiffness of comb-branched polymers. Polym J. 2001;33:874–8.
11. Feuz L, Leermakers FAM, Textor M, Borisov O. Bending rigidity and induced persistence length of molecular bottle brushes: a self-consistent-field theory. Macromolecules. 2005;38:8891–901.
12. Rice SA, Nagasawa M. Polyelectrolyte Solutions. New York: Academic Press; 1961.
13. Oosawa F. Polyelectrolytes. New York: Marcel Dekker; 1971.
14. Rühe J, Ballauff M, Biesalski M, Dziezok P, Gröhn F, Johannsmann D, et al. Polyelectrolyte brushes. Adv Polym Sci. 2004;165:79–150.
15. Kanemaru E, Terao K, Nakamura Y, Norisuye T. Dimensions and viscosity behavior of polyelectrolyte brushes in aqueous sodium chloride. a polymacromonomer consisting of sodium Poly(styrene sulfonate). Polymer. 2008;49:4174–9.
16. Sugiyama M, Nakamura Y, Norisuye T. Dilute-solution properties of polystyrene polymacromonomer having side chains of over 100 monomeric units. Polym J. 2008;40:109–15.
17. Vink H. A new convenient method for the synthesis of poly (styrenesulfonic acid). Macromol Chem Phys. 1981;182:279–81.
18. Hirose E, Iwamoto Y, Norisuye T. Chain stiffness and excluded-volume effects in sodium Poly(styrenesulfonate) solutions at high ionic strength. Macromolecules. 1999;32:8629–34.
19. Takahashi A, Kato T, Nagasawa M. The second virial coefficient of polyelectrolytes. J Phys Chem. 1967;71:2001–10.

20. Benoit H, Doty P. Light scattering from non-gaussian chains. J Phys Chem. 1953;57:958–63.
21. Konishi T, Yoshizaki T, Saito Y, Einaga Y, Yamakawa H. Mean-square radius of gyration of oligo- and polystyrenes in dilute solutions. Macromolecules. 1990;23:290–7.
22. Terao K, Hokajo T, Nakamura Y, Norisuye T. Solution properties of polymacromonomers consisting of polystyrene. 3. Viscosity behavior in cyclohexane and toluene. Macromolecules. 1999;32:3690–4.
23. Hokajo T, Terao K, Nakamura Y, Norisuye T. Solution properties of polymacromonomers consisting of polystyrene V. Effect of side chain length on chain stiffness. Polym J. 2001;33:481–5.
24. Iwamoto Y, Hirose E, Norisuye T. Electrostatic contributions to chain stiffness and excluded-volume effects in sodium Poly(styrenesulfonate) solutions. Polym J. 2000;32:428–34.
25. Yamakawa H, Yoshizaki T. Helical Wormlike Chains in Polymer Solutions. 2nd edn. Berlin Heidelberg: Springer-Verlag; 2016.
26. Domb C, Barrett AJ. Universality approach to the expansion factor of a polymer chain. Polymer. 1976;17:179–84.
27. Abe F, Einaga Y, Yoshizaki T, Yamakawa H. Excluded-volume effects on the mean-square radius of gyration of oligo- and polystyrenes in dilute solutions. Macromolecules. 1993;26:1884–90.
28. Nakamura Y. Stiffness parameter of brush-like polymers with rod-like side chains. J Chem Phys. 2016;145:014903.
29. Manning GS. Limiting laws and counterion condensation in polyelectrolyte solutions. J Chem Phys. 1969;51:924–33.
30. Debye P, Hückel E. Zur Theorie der Elektrolyte. I. Gefrierpunktserniedrigung und verwandte Erscheinungen. Phys Z. 1923;24:185–206.
31. Donnan FG. The theory of membrane equilibria. Chem Rev. 1924;1:73–90.